Vectorial method used to monitor an evolving system: Titanium oxide thin films under UV illumination

Solène Béchu, Bernard Humbert, Vincent Fernandez, Neal Fairley, Mireille Richard-Plouet

Vectorial method used to monitor an evolving system: Titanium oxide thin films under UV illumination

Solène Béchu [a,*], Bernard Humbert [a], Vincent Fernandez [a], Neal Fairley [b], Mireille Richard-Plouet [a,*]

[a] Institut des Matériaux Jean Rouxel (IMN), Université de Nantes, CNRS, 2 rue de la Houssinière, BP 32229, 44322 Nantes cedex 3, France
[b] Casa Software Ltd, 5 Grosvenor Terrace, Teignmouth TQ14 8NE, United Kingdom

Under *in situ* UV illumination, some materials present evolution of their opto-electronic properties that can be monitored by spectroscopy. We present here a mathematical method which can be applied to spectroscopic measurements when an evolving set of data is recorded: the vectorial method. The inves-tigations and quantifications are performed by Infrared spectroscopy and XPS on organic-inorganic thin films prepared by sol-gel. The inorganic part of these hybrid thin films contains Ti oxide-network based whereas the organic part is composed of N,N-dimethylformamide and its hydrolysis products. Under UV illumination, those films exhibit intermediate bandgap behavior due to the photoreduction of Ti(IV) in Ti (III). The role of the solvent in the thin film is underlined during the process of photoreduction together with an understanding of the condensation of the Ti oxide-based network, as these evolutions are critical for the opto-electronic properties of those thin films.

1. Introduction

Over the last decade, a new generation of solar cell was intensively described in the literature. This third generation aims at overpassing the Shockley-Queisser theoretical limit of efficiency conversion which is 31% for a single junction solar cell [1]. Several solutions were proposed such as quantum dot solar cells, tandem solar cells, up and down conversion solar cells and intermediate band solar cells. The later concept was first described by Luque and Marti [2] and consists in introducing an intermediate level in the bandgap of the absorber material. Thanks to this intermediate band, the absorption range becomes wider, due to new absorption processes (valence band-intermediate band and intermediate band-conduction band). Several investigations were performed to identify materials presenting this feature. Among those materials, one hybrid sol-gel, based on titanium oxide, presents some interesting characteristics and was already described in the literature [3–6]. Under UV illumination, an intermediate band appears inside the band gap, in a reversible way, related to the reduction of Ti(IV) to Ti(III), the different Ti oxidation degrees present in the film. Photons with energy at least equal to the band-gap leads to the generation of a hole-electron pair. Since the bottom of Ti oxide conduction band mainly consists in 3d orbitals of the cation, the photogenerated electron stabilizes one of the T_{2g} orbital. This feature is associated with the appearance of a level below the conduction band [7]. However, this is associated to modifications in the organic and inorganic parts of the sol-gel. To evaluate this impact, we decided to follow the progress of the changes via two spectroscopic experiments on hybrid thin films prepared from aged-sols. First, the evolution of the organic part was measured via Infrared analysis under *in situ* UV illumination. Secondly, a similar experiment was run (*in situ* UV illumination) in XPS, in order to understand how the inorganic part of the Ti-oxide network is impacted by the intermediate band appearance. In order to go further in the analytical process we undertook an innovative method of treatment: the vectorial method. This mathematical method was first described in 2015, by Baltrusaitis et al. [8] and then successfully applied to graphite supported copper nanoparticles [9]. Thanks to this method, it is possible to obtain information without any *a priori* prerequisite in a set of evolving data and to mathematically create spectra which were not experimentally reachable. The principle is to extract mathematical vectors with a physical meaning that can reproduce a whole set of data, through linear combinations of the mathematical vectors. The latter have to be identified in a full set of vectors from a weighted difference between two experimental spectra denoted S_i and S_f (Fig. 1) presenting an evolution (S_i and S_f stand for initial and final spectra). Actually, among those vectors, for defined weighted factors α and β, it is possible to find two vectors such as A and B in Fig. 1

* Corresponding authors.
E-mail address: solene.bechu@univ-nantes.fr (S. Béchu).

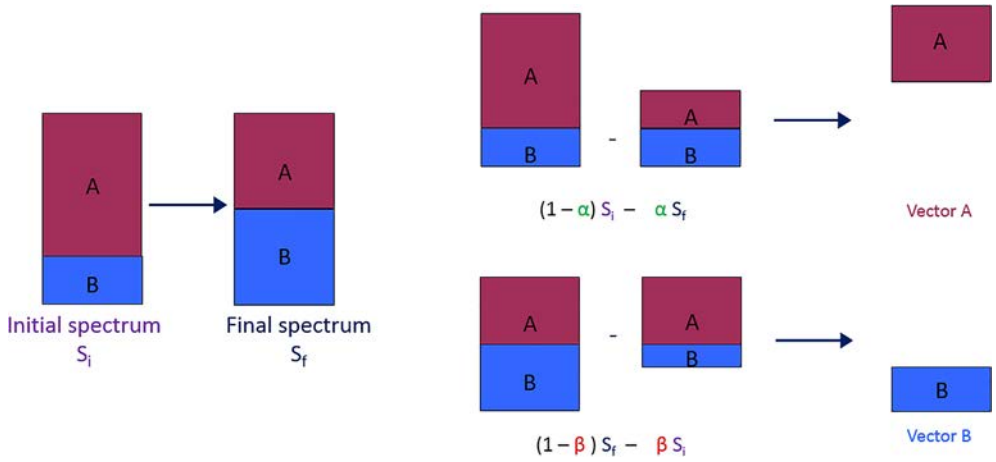

Fig. 1. Schematic view of the vectorial method processing.

which, once linearly combined together, will account for all the experimental set of data. Picking the different vectors requires logic. Indeed, vectors should present coherent spectroscopic evolutions (only positive bands or peaks) and information (existing bands or peaks).

This paper deals with the vectorial method applied to hybrid organic-inorganic films evolving under UV illumination to quantify changes in the inorganic and organic parts of thin films. The vectorial method was so far applied to XPS data only, however, here, we report that it can also successfully be applied to Infrared spectroscopy.

2. Material and methods

2.1. Synthesis

The mechanism of titanium oxide sol and gel (hereafter denoted TiDMF) formation was already detailed in previous studies [3,5]. In a typical experiment, the hybrid organic-inorganic sol is prepared by adding 12 mL of N,N-dimethylformamide (DMF, Carlo Erba, synthesis grade) drop by drop to 5 mL of ice-cooled $TiOCl_2.1.4HCl.7H_2O$ (4.85 mol L^{-1} in titanium, Millennium Chemicals) solution to reach a concentration of 1.42 mol L^{-1}. The reaction mixture is then heated at 70 °C for 20 hours until a viscous and transparent aged-sol is obtained. The advancement of the reaction is monitored by Raman diffusion, until 3.4 DMF per Titanium were hydrolyzed as dimethylammonium chloride (DMACl) and methanoic acid (HCOOH). This equilibrium value originates from the composition of the titanium oxychloride. The aged-sol is then redispersed in the solvent to reduce the viscosity (typically 2 mL of aged-sol in 6 mL of DMF) in order to manage the thickness of the films.

2.2. Films preparation

Films were prepared by spin coating on reflective p-doped silicon for Infra-Red analysis in diffuse reflection mode and UV transparent glass substrates for *in situ* XPS analysis to allow illumination from the bottom side (cf XPS experimental description). After ultrasonication for 5 min with deionized water (removal of dust), ethanol (removal of grease) and isopropanol (pre-treatment for UV-ozone) respectively, substrates are treated under UV-ozone for 10 min to improve wettability of TiDMF aged-sol. Thicknesses of 1 μm were reached by spin coating TiDMF sol, by using the following program: 2 min 3000 rpm and 2 min 4000 rpm. Thicknesses were controlled using a profilometer Dektak 8 (Bruker Nano).

2.3. Infrared analysis

Infrared measurements were performed on a Fourier Transform spectrometer Bruker Vertex 70, using a Praying Mantis diffuse reflection setup to collect diffuse reflectance spectra. Moreover, to control the environment around the samples, they were set in a Harrick HVC accessory under different atmospheres (ambient, dry and secondary vacuum of 5×10^{-4} Pa), for an equilibrium time of 30 min minimum. The chamber was equipped with three optical windows: two infrared transparent windows to allow collecting the Infrared excitation and the Infrared reflectance signals and the third visible transparent silica window to allow *in situ* continuous UV illumination (led emitting at 365 nm). Infrared spectral measurements were recorded every five minutes for the first 30 min, then every 10 min. We recorded the infrared spectra of samples without any mixing with another non-infrared-absorbent matrix allowing us to avoid any surface modifications. A DTHS detector and a KBr beam splitter in the Michelson interferometer were used for both spectral ranges NIR (8000–4000 cm^{-1}) and MIR (4000–400 cm^{-1}). For each sample, at least 20 scans with a spectral resolution of 4 cm^{-1} were recorded. The sample spectra obtained by this technique are presented in this work as the result of the subtraction of the original spectrum and that of a reference. The pseudo absorbance is plotted as log (R_{sample}/R_{ref}) where R_{sample} and R_{ref} are respectively the diffuse single-beam reflectance of the sample and the reflectance reference.

2.4. XPS analysis

XPS measurements were performed on a Kratos Axis Ultra and on a Kratos Axis Nova spectrophotometers using a monochromatic Al Kα source 1486.6 eV operating at 150 W, with charge neutralizer. Survey spectra were recorded at a pass energy of 160 eV corresponding to an all over instrument resolution measured on Silver Fermi edge of 1.95 eV and a step of 1 eV from -5 to 1350 eV. High resolution spectra of O 1 s, Ti 2p, N 1 s, C 1 s, and Cl 2p core levels were recorded with an all over instrument resolution measured on Silver Fermi of 0.53 eV and a step of 0.1 eV at a pass energy of 40 eV. To perform the *in situ* illumination, samples of TiDMF were placed on a dedicated sample holder with an incorporated UV led (emitting at 375 nm with a 3.2 mW cm^{-2} power density) [6]. The bottom side of the films are illuminated through a UV transparent substrate. Calibrations were performed on Cl 2p3/2 peak (197.9 eV) since it is the only peak which does not present any position evolutions during illumination, with only one chloride chemical environment for all measurements. All spectra were fit-

ted using a U2 Tougaard function for the background and with a pseudo-Voigt function with a Lorentzian ratio of 50% for the various peaks.

2.5. Data processing

All spectra (Infrared and XPS spectra) were handled with the software CasaXPS (version 2.3.18) [10]. The vectorial method is applied to the initial spectrum (S_i) and the final one (S_f) according to the equation $X_j = (1 - c_j)S_i - c_jS_f$ with c_j varying between 0 to 1 by step scan of F/100, with F the chosen factor. Consequently, j is an integer varying between 0 and 100/F. The vectorial method is available in the menu Options, by activating in Spectrum Processing the tab Calculator and by choosing a specific Factor F (0.5 for Infrared measurements and 1 for XPS ones), for two spectra of interest (usually one at the beginning of the evolution and one at the end). Once the vectors are generated, two or more have to be carefully identified to account for the evolution of the set of spectra.

3. Results and discussion

3.1. Infrared analysis of TiDMF thin films

The description of Infrared vibrations has already been reported in the literature [3] for the TiDMF material. Once deposited as thin films, no evolution in the Infrared vibrations was detected: same species (DMF, DMACl, HCOOH, $HCOO^-$ and H_2O) can be found in the different spectra. The photo-reduction was run under several atmospheres, to explore the difference with ultra-vacuum in the XPS chamber. In the different atmospheres tested (ambient, dry, and secondary vacuum), we noticed that the vibrations impacted by the illumination are linked to the following species: DMACl, HCOOH and $HCOO^-$ (Fig. 2 a.), which partially disappear. However, it is not possible to obtain a quantification of this impact due to the DMF loss. Because a condensation of the network occurs during pre-heating treatment to get a sol suitable for processing by spin coating, part of DMF molecules are enclosed but not linked to the solid part of the sol, during spin-coating, they are expelled from the film. Actually, during the deposition process of TiDMF, it was seen (by Raman analyses) that a significant amount of DMF is lost. Moreover, at the end of the experiment, we need to get the amount of photo-reduced species but there is no experimental method to get the totally reduced spectrum. Therefore, we propose to get it through a mathematical way.

3.1.1. Vectorial method applied to Infrared spectra

In order to get quantified results, the vectorial method was applied to the whole dataset of spectra. Through this process, 200 X_j vectors are generated. In order to precisely detect which vibrational bands are impacted by the photoreduction, the X_{100} vector ($c_j = 0.5$) corresponding to the difference between the initial

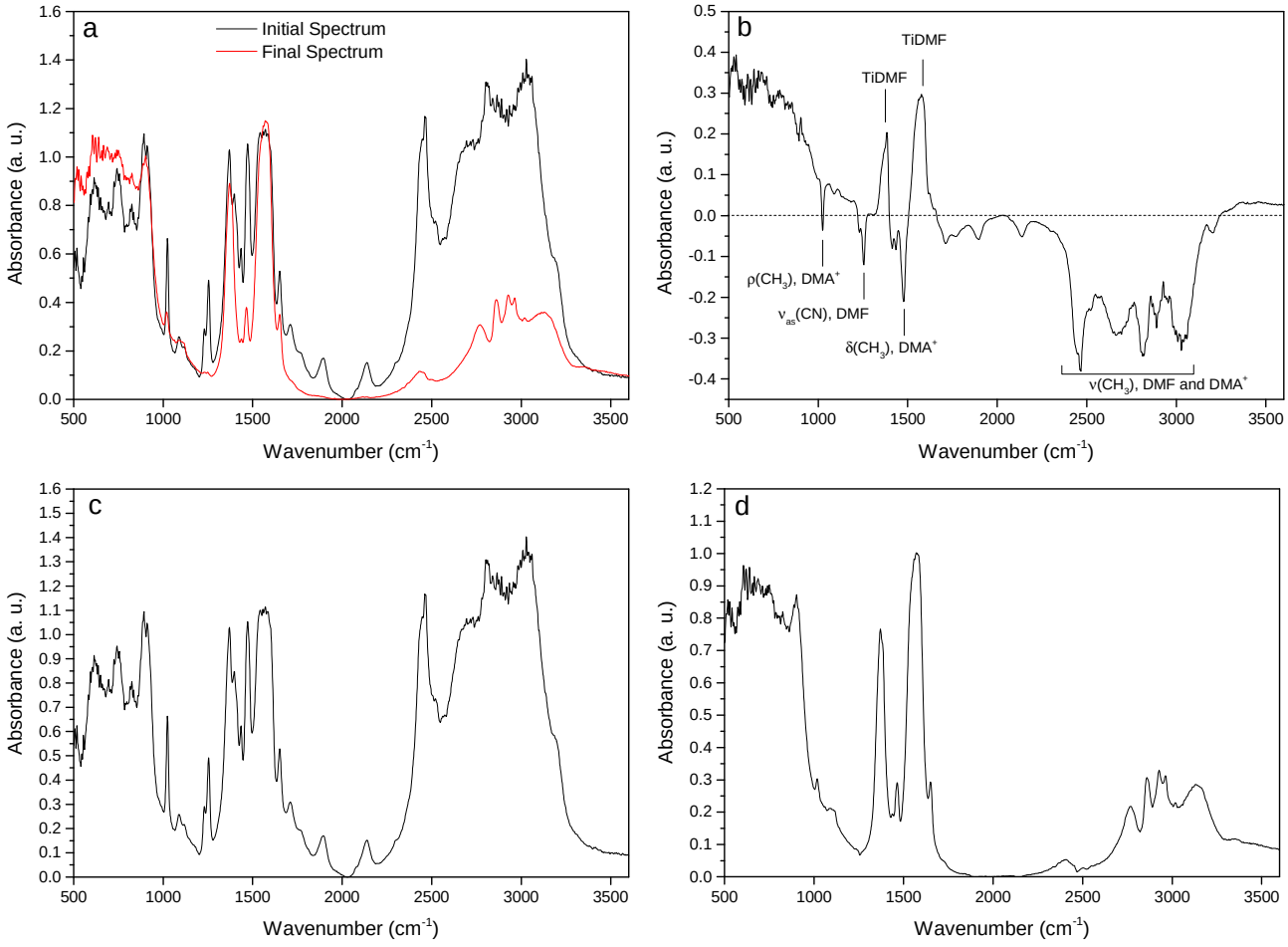

Fig. 2. Infrared spectra of TiDMF layer before illumination (black) and after 4 h (red) of illumination under secondary vacuum (5.2×10^{-4} mbar) (a); X_{100} vector, positive signals increase in the corresponding species, negative signals: decrease in the corresponding species under secondary vacuum (b); Pristine vector obtained for a TiDMF layer under secondary vacuum (c); Totally reduced vector ($X_{93.5}$) obtained for a TiDMF layer under secondary vacuum (d). (For interpretation of the references to colour in this figure legend, the reader is referred to the web version of this article.)

and the final spectra is examined. It allows the identification of the vibrations evolving from the initial to final spectra (Fig. 2b). In this difference, bands showing a negative absorbance are attributed to disappearing species upon illumination and those with a positive absorbance are corresponding to species formed upon illumination.

Regarding these evolving signals, it is possible to check that the pristine vector (non-impacted by the reduction) is the first vector obtained by the vectorial method. Indeed, in the peculiar case, it corresponds to the equation where the coefficient c_j is equal to 0, so to the initial spectrum, which was not impacted by the reduction (Fig. 2c). Absorption signal corresponding to this vector are composed of DMF, DMACl, HCOOH and $HCOO^-$.

The totally reduced vector is then chosen among the set of vectors generated during the application of the vectorial method and corresponds to j = 93.5. It has to mainly present the vibrations of DMF since the species impacted by reduction are DMACl and HCOOH. It also has to display a physical meaning, with bands presenting a positive absorbance (Fig. 2d). The vector 93.5 was favored to the detriment of vector 93 due to the fact it is the first one with a physical meaning. The vector 94 could also have been used to describe the system, leading to similar percentage of reduction after the same amount of reduction time.

Then, both overall spectra are defined as a user-defined lineshape and will be used to describe the whole infrared data set. By combining those two components (pristine vector and totally reduced vector) coherent fits are obtained for all the different spectra from the original evolving set (Fig. 3 a.), reaching 89% of reduction after 4 h of illumination under secondary vacuum.

Through this decomposition, the evolution of the data set can be followed (Fig. 3 b.). For a same time of illumination (3h30), the impact of the different atmospheres can be assessed. The presence of water limits the reduction of the TiDMF layer, as it can be seen by comparing the percentage of reduction under ambient and dry atmospheres (32% vs 42% for 3 h30 of illumination). Under secondary vacuum, the percentage of reduced vector is far more important than under a dry or an ambient atmosphere (86% for 3 h30 of illumination).

3.1.2. Correlation with XPS measurements

In order to check the validity of this approach, the spectra of the films illuminated under ambient and dry atmospheres were measured by XPS. This measurement led to the percentage of reduction of Ti(IV) in Ti(III), which will then be correlated to the percentage of the reduced vector used in the vectorial method. XPS measurements show 43% and 46% of Ti(III) (Fig. 3c) for film illuminated under ambient or dry atmosphere, respectively. This is coherent with the amount evaluated by the vectorial method applied to the infrared data (Table 1).

Species impacted by the reduction are evacuated under secondary vacuum and cannot condense again on the surface of the film. Water and the non-evacuation of impacted species (DMACl

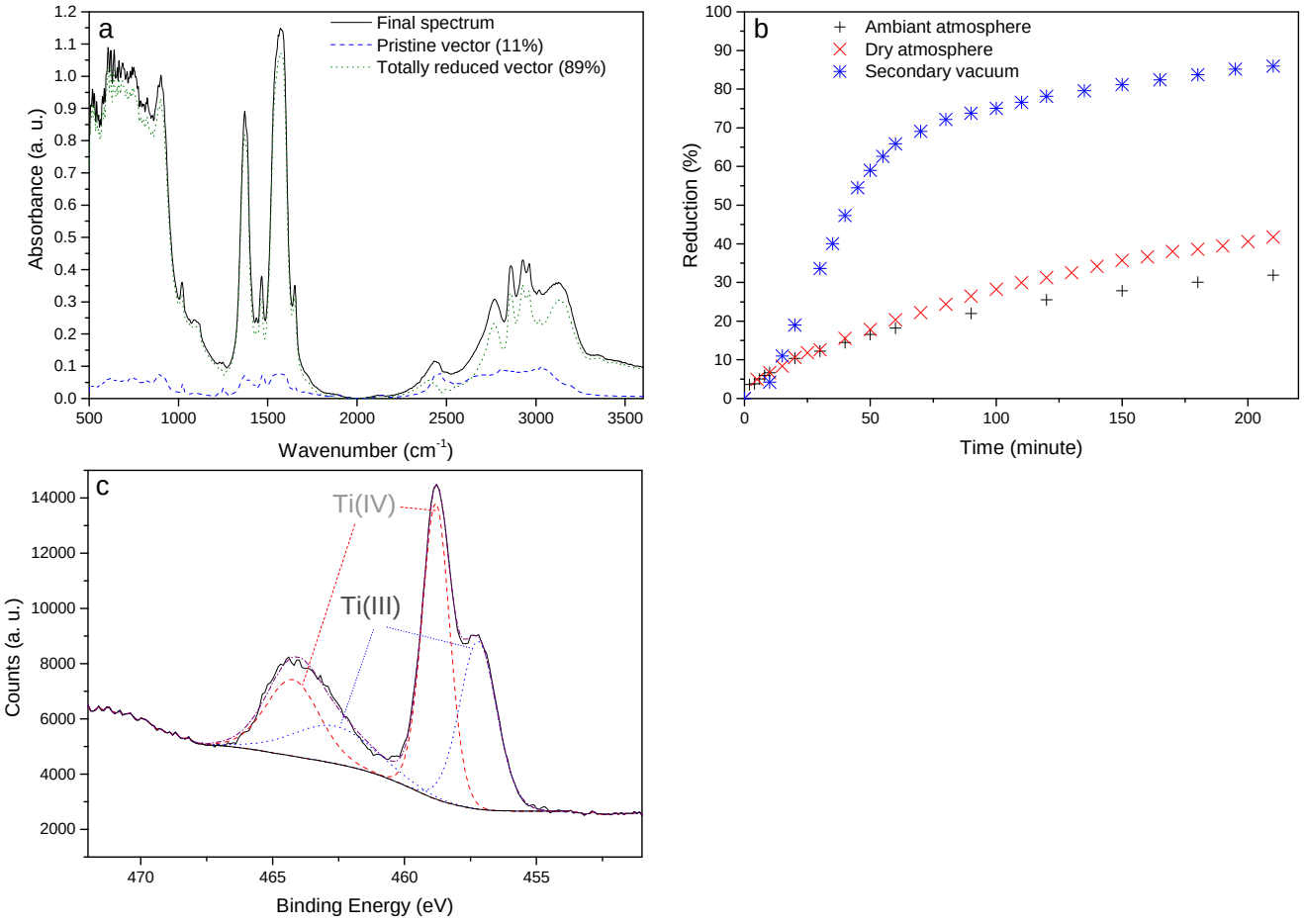

Fig. 3. Infrared spectrum after 4 h of illumination (line)) with its decomposition (pristine vector in dash and totally reduced vector in dot) under secondary vacuum atmosphere (a.); Evolution of the reduced vector percentage in the Infrared spectra fits under different atmospheres (b.); XPS spectrum of Ti 2p for an TiDMF layer reduced for 5 h30 with the contribution of Ti(IV) and Ti(III) under ambient atmosphere (c.) (For interpretation of the references to colour in this figure legend, the reader is referred to the web version of this article.)

Table 1
Percentage comparison of reduced part generated under UV illumination (5 h 45 min for ambient atmosphere and 3 h 30 min for dry atmosphere) obtained by vectorial method and XPS measurements.

	$\%_{\text{reduced vector}}$ (Vectorial method)	$\%_{\text{Ti(III)}}$ (XPS measurements)
Ambient atmosphere	41%	43%
Dry atmosphere	46%	46%

and HCOOH) can be inferred as critical to obtain high percentages of reduction.

Due to the experimental constrains related to pressure rising, films illuminated under secondary vacuum could not be run for XPS measurements. However, an *in situ* illumination was performed to determine the maximal percentage of reduction. For 13 h of illumination, up to 20% of Ti(IV) was reduced in Ti(III). The important difference between both conditions is due to the difference in pressure and its impact on the material. Indeed, during XPS measurements, the vacuum reached about 10^{-8} Pa. Under this pressure, all non-bounded DMF evaporates from the thin film while not under secondary vacuum (Supporting info, Fig. 1). We then deduce that to obtain high reduction ratio, films must contain some DMF.

3.2. XPS analysis on TiDMF thin films

3.2.1. Vectorial method applied to XPS spectra

To complete the results, the vectorial method was also used to identify the evolution of the inorganic part of the hybrid films. Similarly to Infra-Red experiments, *in situ* UV illumination was performed in the XPS chamber. XPS measurements show a small shift (0.3 eV) of the titanium 2p peak after a certain amount of *in situ* reduction (Fig. 4a) while the O 1s spectra do not present any energy shift (Fig. 4b).

Two states can be defined inside the system: a certain percentage of non-reduced TiDMF (Ti(IV)) and a percentage of reduced TiDMF (equivalent to the apparition of Ti(III)). However, the shift in the Ti(IV) peak implies a change in the structure of the layer. In order to understand this structural change, the vectorial method was applied to Ti 2p and to O 1 s combined spectra, species which are well impacted by the illumination. Spectra merging was performed in Casa XPS (Spectrum Processing/test data/merge irregular) for analyzing correlated chemical core levels and allowing more precision over the reduced vector choice. The pristine vector characterizes the state of non-reduced TiDMF whereas the reduced vector defines the state of reduced TiDMF. Once again, it is possible to observe which peaks will be impacted by the reduction. In Fig. 4c., examination of the X_{49} vector (difference between the initial and final spectra) allows us to confirm that, as expected, the Ti (III) peak is increasing to the detriment of Ti(IV) peak. Moreover, this evolution is associated to an increase in the O 1 s component associated to Ti-**O**-Ti bonds at 529.7 eV [11] to the detriment of Ti-**O**-X, X = C or H at 531.4 eV [12–15]. It has been noticed that the contribution of Ti(III) generated presents a full width at half maximum (fwmh) too important (2.49 eV) to be correlated to one component only. Two contributions of Ti(IV) are then be considered, which leads to two contributions of Ti(III): Ti out (III) will

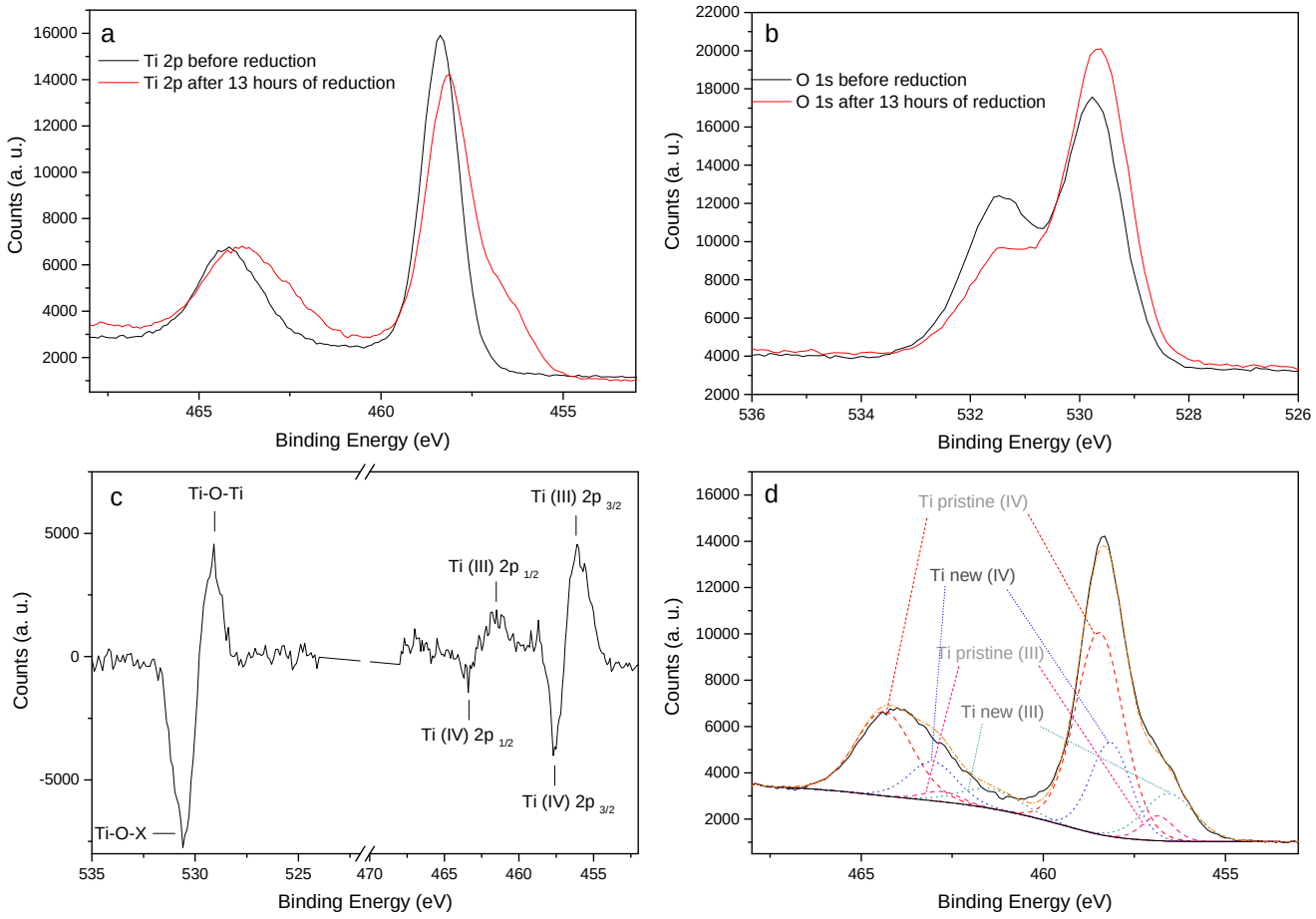

Fig. 4. Ti 2p spectra before (black) and after (red) 13 h of reduction (a.); O 1 s spectra before (black) and after (red) 13 h of reduction (b.); Vector X_{49} showing the peaks evolutions under reduction (positives ones: increasing, negatives one: decreasing) (c.); Final Ti 2p spectrum fitted with all the contributions (d.) (For interpretation of the references to colour in this figure legend, the reader is referred to the web version of this article.)

Table 2
ligand numbers before and after *in situ* illumination with ε, number of ligands, χ, number of μ_3 type ligands and ω, number of μ_2 type ligands.

	Non illuminated aged-sol	Illuminated aged-sol
Formulation	$TiO_{1.43}(HCOO)_{0.57}(OH)_{0.57}$	$Ti(IV)_{0.80}Ti(III)_{0.20}O_{1.43}(HCOO)_{0.25}(OH)_{0.69}$
ε	2.57	2.37
χ	2.6	3.8
ω	3.4	2.2

be located at the edge of the material network while Ti in (III) is in the core of the network.

3.2.2. Evolution of the contributions

The first position of Ti(IV) is the usual one, at 458.4 eV 16,17, while the new position (obtained through the vectorial method) is shifted at 458.1 eV. Once those positions are defined, the XPS spectra are fitted with those two positions of Ti(IV), correlated with two positions of Ti(III) at 457.1 and 456.7 eV [16,17]. Fitting of the different spectra are performed by using those 4 contributions in Fig. 4d. Evolution of Ti (IV) components (Supporting information, Fig. 2) shows that the usual contribution of $Ti_{pristine}$ (IV) decreases with UV illumination time while the Ti_{new} (IV) one obtained via the vectorial method increases up to 10%. To discriminate each position of Ti(IV) in the network, the previous results have to be correlated with the evolution of O 1 s contributions. During the UV illumination, the contribution of Ti-**O**-X at 531.4 eV decreases while the Ti-**O**-Ti one at 529.7 eV increases, which is in correlation with the results of the vectorial method as it shows that the contribution of Ti-**O**-X decreases over time. Through those data, it can be considered that the $Ti_{pristine}$ (IV) at 458.4 eV is located at the edge of the material network because it evolves coherently with Ti-**O**-X oxygen species. On the contrary, the Ti_{new} (IV) observed thanks to the vectorial method is in the core of the network and is engaged in a Ti-**O**-Ti framework as it is a signature of the oxide network appearing during the condensation of the network upon illumination. Ti_{out} (III) and Ti_{in} (III) contributions follow similar behavior as $Ti_{pristine}$ (IV) and Ti_{new} (IV) respectively.

3.3. Network condensation

Moreover, over the illumination time, this condensation is also noticed through the XPS global formulations. Before UV illumination, the formulation of film is $Ti(IV)O_{1.43}(HCOO)_{0.57}(OH)_{0.57}$ + 0.12 DMACl + 0.06 DMA + 0.20Cl^-. After UV illumination, the formulation becomes $Ti(IV)_{0.80}Ti(III)_{0.20}O_{1.43}(HCOO)_{0.25}(OH)_{0.69}$ + 0.04 DMACl + 0.03 DMA + 0.14Cl^-. Thanks to those formulations, an average representation of the titanium oxide network is obtained. The generic formulation of the layer is $TiO_{n-z}(OH)_{4-2n+z}(HCOO)_z$ with n value between 0 and 2. The z coefficient is obtained from the number of methanoates from C1s contribution at 288.3 eV [12,13]. This equilibrated reaction releases z protons H^+ which interact with the oxygen connected to titanium, leading to hydroxyls ions. Previous results [3] proved that the titanium cation sits in an octahedral environment and is linked to 6 oxygenated ligands. The global formula is then TiL_ε, with L representing oxygen, hydroxyls and methanoates and ε value ranging between 2 and 3. Actually, two extreme cases exist; the first one corresponds to ε = 2, i.e. each ligand is a μ_3-type (χ) (like in TiO_2), linked to the metal via three bonds and counted for one third per Ti atom. When ε = 3 (second extreme case), each ligand is a μ_2-type (ω), linked to the metal via two bonds and counted for one half per Ti atom (like in the perovskite $CaTiO_3$, octahedra are sharing corners only). From the generic formula, the ligands number (ε) can be obtained with the following equation: $\varepsilon = n - z + 4 - 2n + z + z = 4 - n + z$. From the following equations, quantities of μ_3-type (χ) and μ_2-type (ω) ligands can be determined.

$$\varepsilon = n - z + 4 - 2n + z + z = 4 - n + z$$

$$\omega = 6\varepsilon - 12 = 6(2 - n + z)$$

$$\omega + \chi = 6$$

$$\varepsilon = \frac{\chi}{3} + \frac{\omega}{2}$$

Over illumination, the network condensates since the number χ of μ_3-type ligands increases to the detriment of μ_2-type ligands (Table 2).

From those data, it is possible to construct an average representation of an octahedron (Fig. 5). Infrared measurements show that methanoates species are μ_2-type [18]. To obtain a coherent stoichiometry, they are completed with hydroxyl ligands, whereas oxygens are considered as μ_3-type. Red bonds represent μ_2-type ligands whereas μ_3-type ligands are represented by green bonds. Black bonds depict a hybrid behavior, where the bond implies two or three metallic cations with a percentage corresponding to each type of connection.

4. Conclusions

The appearance of the intermediate band in the material leads to several important changes in the titanium oxide based nanomaterial. The vectorial method was successfully applied to Infrared spectra obtained under *in situ* UV illumination in different atmospheres, allowing to get the percentage of reduction of the thin films. We also proved here that presence of water plays an impor-

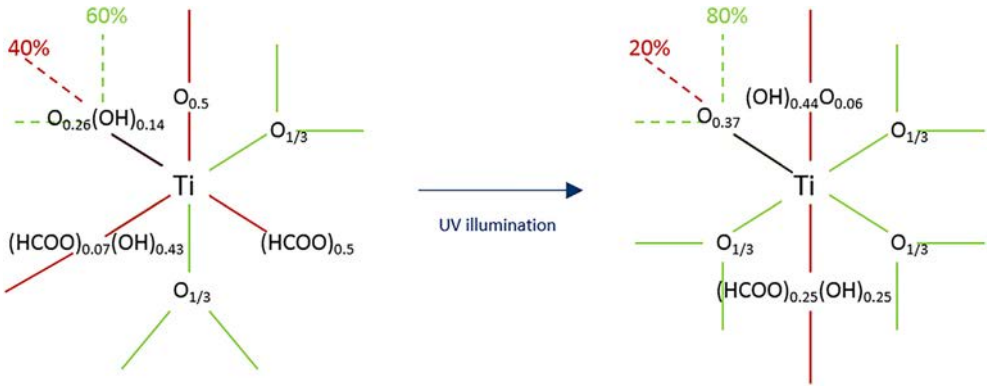

Fig. 5. Average representations before (left) and after (right) UV illumination.

tant part in the mechanism of reduction, by inhibiting the photoreduction. By comparing infrared and XPS measurements, the role of DMF was also underlined in the percentage of reduction of the system, as its presence leads to higher percentages of reduction. Moreover, a condensation of the network is observed, which can be linked to the expulsion of organic species (DMA^+ and HCOOH) from the structure. Thanks to the vectorial method, investigations lead to a better understanding of the mechanism of network condensation, including the appearance of a new position in the titanium XPS signals. Combining experimental data to vectorial method led to interesting results. Together with other separation source methods (PCA [19], BSS [20] for instance), the vectorial method is easy to handle to point out and identify variability in a whole data set.

References

[1] W. Shockley, H.J. Queisser, J. Appl. Phys. 32 (3) (1961) 510.
[2] A. Luque, A. Martí, Phys. Rev. Lett. 78 (26) (1997) 5014–5017.
[3] T. Cottineau, M. Richard-Plouet, A. Rouet, E. Puzenat, H. Sutrisno, Y. Piffard, P.-E. Petit, L. Brohan, Chem. Mater. 20 (4) (2008) 1421–1430.
[4] T. Cottineau, L. Brohan, M. Pregelj, P. Cevc, M. Richard-Plouet, D. Arčon, Adv. Funct. Mater. 18 (17) (2008) 2602–2610.
[5] T. Cottineau, M. Richard-Plouet, J.-Y. Mevellec, L. Brohan, J. Phys. Chem. C 115 (25) (2011) 12269–12274.
[6] T. Cottineau, A. Rouet, V. Fernandez, L. Brohan, M.J. Richard-Plouet, Mater. Chem. A 2 (29) (2014) 11499.
[7] M.T. Greiner, M.G. Helander, W.-M. Tang, Z.-B. Wang, J. Qiu, Z.-H. Lu, Nat. Mater. 11 (1) (2012) 76–81.
[8] J. Baltrusaitis, B. Mendoza-Sanchez, V. Fernandez, R. Veenstra, N. Dukstiene, A. Roberts, N. Fairley, Appl. Surf. Sci. 326 (2015) 151–161.
[9] M. d'Halluin, T. Mabit, N. Fairley, V. Fernandez, M.B. Gawande, E. Le Grognec, F.-X. Felpin, Carbon 93 (2015) 974–983.
[10] N. Fairley, Casa Software Ltd.
[11] J.F. Moulder, W.F. Stickle, P.E. Sobol, K.D. Bomben, Handbook of X-ray Photoelectron Spectroscopy, vol. 3; 1992.
[12] L.-Q. Wang, K.F. Ferris, A.N. Shultz, D.R. Baer, M.H. Engelhard, Surf. Sci. 380 (2–3) (1997) 352–364.
[13] M.R. Alexander, G. Beamson, C.J. Blomfield, G. Leggett, T.M.J. Duc, Electron Spectrosc Relat. Phenom. 121 (1–3) (2001) 19–32.
[14] J.C. Yu, L. Zhang, Z. Zheng, J. Zhao, Chem. Mater. 15 (11) (2003) 2280–2286.
[15] Y. Gao, Y. Masuda, K. Koumoto, Langmuir 20 (8) (2004) 3188–3194.
[16] A.N. Shultz, W. Jang, W.M. Hetherington, D.R. Baer, L.Q. Wang, M.H. Engelhard, Surf. Sci. 339 (1–2) (1995) 114–124.
[17] F. Guillemot, M. Porté, C. Labrugère, C. Baquey, J. Colloid Interface Sci. 255 (1) (2002) 75–78.
[18] K. Nakamoto, Infrared and Raman Spectra of Inorganic and Coordination Compounds, vol. 85, 1986.
[19] V.H. Segtnan, S. Sasic, T. Isaksson, Y. Ozaki, Anal. Chem. 73 (13) (2001) 3153–3161.
[20] M. Toiviainen, F. Corona, J. Paaso, P. Teppola, J. Chemom. 24 (7–8) (2010) 514–522.